MAXIMUM BRIGHTNESS OF LINAC-DRIVEN ELECTRON BEAMS IN THE PRESENCE OF COLLECTIVE EFFECTS

S. Di Mitri†, Elettra – Sincrotrone Trieste S.C.p.A., Basovizza, Trieste I-34149

Abstract

Linear accelerators capable of delivering high brightness electron beams are essential components of a number of research tools, such as free electron lasers (FELs) and elementary particle colliders. In these facilities the charge density is high enough to drive undesirable collective effects (wakefields) that may increase the beam emittance relative to the injection level, eventually degrading the nominal brightness. We formulate a limit on the final electron beam brightness, imposed by the interplay of geometric transverse wakefield in accelerating structures and coherent synchrotron radiation in energy dispersive regions. Numerous experimental data of VUV and X-ray FEL drivers validate our model. This is then used to show that a normalized brightness of 10^{16} A/m^2, promised so far by ultra-low charge beams (1-10 pC), can in fact be reached with a 100 pC charge beam in the Italian FERMI FEL linac, with the existing machine configuration.

INTRODUCTION

In this article we recall a limit on the maximum brightness of an ultra-relativistic electron beam achievable in a single-pass linac when collective effects are part of the dynamics [1]. The limit is determined by the interplay of the dispersion strength (*e.g.*, bunch length compression factor) with the linac geometric transverse wakefield (GTW) and coherent synchrotron radiation (CSR) effect on the transverse emittance. We validate our model by means of a systematic comparison of theoretical predictions with experimental data in the linac of FERMI FEL [2-4]. We show that the effects of GTW and CSR on the final beam quality, which has traditionally been treated separately in the archival literature, are coupled by the variation of the bunch length along the beam line. Hence, GTW and CSR should be considered simultaneously during machine design.

Without aiming to replace powerful and sophisticated numerical codes, the analysis proposed in this paper purports to be useful as an exploratory and fast tool to maximize the beam brightness. It is worth to mention that, in principle, the brightness can always be improved by brute force, *e.g.* increasing the beam energy, thus with a direct impact on the accelerator size and cost. Our analysis, instead, aims to maximize the brightness by improving the accelerator performance once the beam line is given, thus with no additional costs.

MODELLING COLLECTIVE EFFECTS

By using the beam matrix formalism, one finds that the CSR-induced normalized emittance growth in the bending plane is [5]:

$$\Delta\gamma_0\varepsilon_{i,0} \cong \gamma_0\varepsilon_{i,0}\left[\sqrt{1+\frac{\breve{\beta}\theta^2\sigma_{\delta,CSR}^2}{\varepsilon_{i,0}}}-1\right] \equiv \gamma_0\varepsilon_{i,0}\left[\sqrt{1+X_{CSR}}-1\right], \quad (1)$$

where γ_0 and $\varepsilon_{i,0}$ are, respectively, the relativistic Lorentz factor and the unperturbed geometric emittance at the dispersive insertion, θ is bending angle, $\breve{\beta}$ is the minimum value of β in the insertion, and $\sigma_{\delta,CSR}$ is the CSR-induced RMS energy spread relative to the beam mean energy. The latter is [6]:

$$\sigma_{\delta,CSR} = 0.2459\frac{r_e}{e}\frac{Q}{\gamma}\left(\frac{l\theta^2C^4}{\sigma_{z,0}^4}\right)^{1/3}, \quad (2)$$

where we introduced the electron classical radius r_e and the electron charge e, Q is the bunch total charge, l the dipole magnet length, $\sigma_{z,0}$ the inital RMS bunch length and C the (linear) compression factor, *i.e.* the ratio of the initial over the final bunch length:

$$C = \frac{\sigma_{z,0}}{\sigma_{z,f}} = \frac{1}{1+hR_{56}} \approx \frac{1}{1+(\sigma_{\delta,0}/\sigma_{z,0})R_{56}}. \quad (3)$$

Here $\sigma_{\delta,0}$ is the relative energy spread imparted to the beam by the upstream RF off-crest acceleration. The longitudinal transport matrix element R_{56} is determined by the dispersive insertion geometry and is, for a four dipoles, achromatic and symmetric chicane with θ<<1, $R_{56} \cong -2\theta^2\left(L_{12}+\frac{2}{3}l\right)$, where L_{12} is the drift length between the two outer bending magnets. In our convention, a negative R_{56} compresses the bunch duration if the linearly correlated energy chirp h is positive.

The single-bunch transverse wakefield instability [7], which happens when the bunch travels at a distance Δ from the linac electric axis, generates a displacement of the trailing particles respect to the bunch head; this displacement is correlated with the longitudinal coordinate along the bunch. The trailing particles start a betatron oscillation around a new dispersive trajectory, therefore increasing their Courant-Snyder invariant. Such an effect can be removed by finding a "golden" trajectory which makes the wakefield's kicks cancel each other (emittance bumps) [8–10]. In analogy with the CSR case, the transverse emittance dilution at the linac end is [9]:

$$\Delta\gamma_f\varepsilon_{f,0} \cong \gamma_f\varepsilon_{f,0}\left[\sqrt{1+2\left(\frac{\pi r_e}{Z_0ce}\right)^2\frac{Q^2\overline{W}_\perp{}^2\Delta^2L_{FODO}L_{tot}\overline{\beta}}{\gamma_f\varepsilon_{f,0}\sqrt{\gamma_0\gamma_f}}}-1\right] \equiv \quad (4)$$
$$\equiv \gamma_f\varepsilon_{f,0}\left[\sqrt{1+X_W}-1\right],$$

where $Z_0 = 377\ \Omega$ is the vacuum impedance, c is the speed of light in vacuum, γ_f and $\varepsilon_{f,0}$ are, respectively, the relativistic Lorentz factor and the unperturbed geometric emittance at the linac end, $\overline{\beta}$ the average betatron function

† simone.dimitri@elettra.eu

along the linac of length L_{tot}, whose accelerating structures have all length $L_{FODO}/2$, Δ is the RMS offset of the randomly displaced accelerating structures, and $\overline{W}_{\perp}$ is the geometric transverse wake function per unit length computed at $z = 2\sigma_z$. The short-range transverse wake function of a cylindrical axis-symmetric structure is given by [7]:

$$W_{\perp}(z) = A\left[1-\left(1+\sqrt{\frac{z}{s_1}}\right)\exp\left(-\sqrt{\frac{z}{s_1}}\right)\right], \quad (5)$$

where A and s_1 depend on the geometry of the accelerating structure's inner cells. If we assume that CSR and GTW kicks are uncorrelated and that the bunch length compression is in one plane only, the final normalized beam brightness is [1]:

$$B_{n,f} \equiv \frac{I}{\gamma_f^2 \varepsilon_{x,f}\varepsilon_{y,f}} = \frac{CI_0}{(\gamma_0\varepsilon_{i,0})^2\sqrt{(1+X_W)(1+X_{CSR}+X_W)}} \equiv \quad (6)$$

$$\equiv \frac{CB_{n,0}}{\sqrt{(1+X_W)(1+X_{CSR}+X_W)}},$$

where $\gamma_f\varepsilon_{f,0} = \gamma_0\varepsilon_{i,0}$ is a constant of motion and we have assumed for simplicity identical unperturbed normalized emittances in the transverse planes. The final normalized brightness $B_{n,f}$ is linearly proportional to the initial normalized brightness $B_{n,0}$, as it comes from the injector, times the compression factor C. We define the brightness *efficiency* as $B_{n,f}/CB_{n,0}$.

MODEL VALIDATION

The theoretical brightness was compared to the experimental one in FERMI over a 250-500pC charge range, and for different bunch lengths. A collection of data and parameters used or the comparison is in Table 1. The result of the comparison is in Fig. 1.

Table 1: FERMI electron beam and accelerator parameters. I_0 is $Q\cdot c$ divided by $3.5\sigma_{z,0}$, where Q is the beam charge and $\sigma_{z,0}$ is the RMS bunch length.

Parameter	FERMI-250	FERMI-500	Units
Q	250	500	pC
$\sigma_{t,0}$	2.4	2.8	ps
I_0	30	50	A
C	7	12	-
γ_0	590	550	-
γ_f	2450	2450	-
L_{FODO}, L_{tot}	12, 45	12, 45	m
$\overline{\beta}$	25	25	m
$\tilde{\beta}$	3	3	m
Δ	200	100	μm
$W_{\perp 0}$	17×10^{16}	17×10^{16}	V/C/m^2
ε_{n0}	1.0	1.0	μm rad
ε_{nf}	2.3	2.0	μm rad
$CB_{n,0}$	2.1×10^{14}	6.1×10^{14}	A/m^2
$B_{n,f}$ (exp.)	0.4×10^{14}	1.5×10^{14}	A/m^2
$B_{n,f}$ (Eq. 6)	0.4×10^{14}	1.7×10^{14}	A/m^2

The GTW is expected to dominate the brightness over the full range of charges. This is depicted by the dash line that describes the theoretical brightness dependence on charge Q and compression factor C when only GTW is considered, shown in Fig. 2.

The uncertainty on the theoretical brightness is dominated by the uncertainty on the linac misalignment (Δ) and the focusing properties ($\overline{\beta}$). Partial suppression of GTW effect is described in our model with an overall smaller misalignment of the linac with respect to the beam reference trajectory. At the end, the analysis is able to predict the effective brightness with an accuracy in the range 10%–20%. Of equal importance as the brightness prediction, the model is able to recognize the dominant degradation source through plots like that one of Fig. 2.

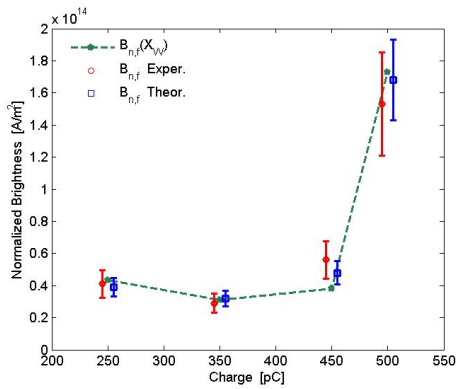

Figure 1: Measured (circles) and predicted (squares) normalized brightness at the end of the FERMI linac as a function of the beam charge. The compression factors are 7, 6, 6 and 12 for beam charge values of 250, 350, 450 and 500 pC, respectively. The compression and charge markers are shifted in the abscissa for better reading. The dash line, which is used to guide the eye, represents Eq. (6) when only GTW is considered. Copyright of American Phys. Society (2013) [1].

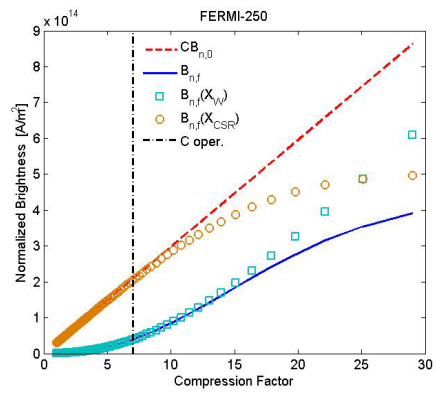

Figure 2: Theoretical final normalized brightness in the FERMI linac as a function of the compression factor, for 250pC beam charge. The nominal (unperturbed) brightness is in dashed line, the effective (perturbed) brightness is in solid line, CSR (circles) and GTW dominated brightness (squares) is also shown. The dash-dot line identifies the operational compression factor. Copyright of American Phys. Society (2013) [1].

MAXIMUM BRIGHTNESS

Figure 3, top plot, shows the brightness of ultra-low charge beams after having been hypothetically accelerated and time-compressed in the LCLS beam delivery system. In all scenarios, the magnetic compression was set for a 1.5 kA final peak current. The CSR wake turns out to be the only important perturbation for these beams since, according to Eq. (2) and Eq. (5), low charge and short duration suppress the GTW instability. A normalized brightness of up to two orders of magnitude higher than what currently achieved in existing facilities appears reachable.

The FERMI-100 case is the result of an optimization of the parameters involved in Eq. (6) that tends to maximize the brightness efficiency $B_{n,f}/CB_{n,0}$, as shown in Fig. 3, bottom plot. This optimized scenario improves the FERMI brightness reported in Table 1 for a charge of 500 pC, by a factor ~100. Although the brightness gain factor of 100 is partly provided by higher initial brightness and compression factor, there is no guarantee *a priori* that GTW and CSR effects, once taken into account, would sustain the same gain. The analysis shows that this is indeed the case, leading to a working point that ensures high brightness efficiency.

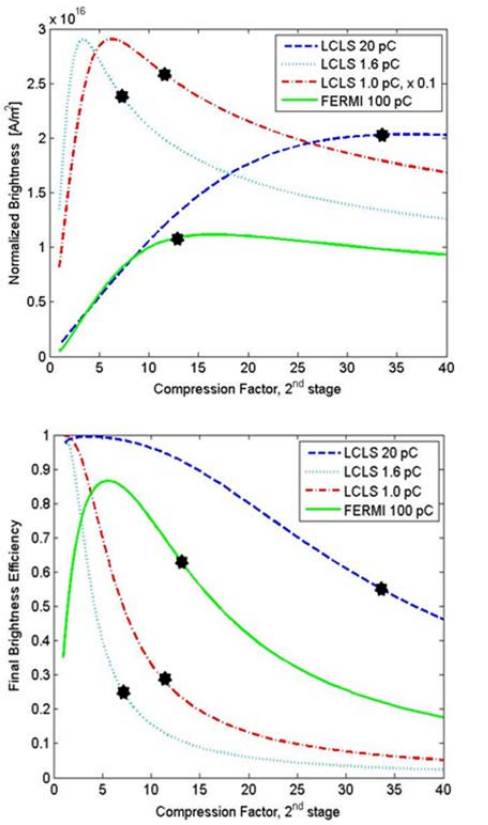

Figure 3: Final normalized brightness (top) and brightness efficiency (bottom) as a function of the compression factor in the second compressor, for the scenarios depicted in Table 2. The star identifies the compression factor that is needed to a reach 1.5 kA final peak current. Copyright of American Phys. Society (2013) [1].

Table 2: Ultra-low charge beam and machine parameters. The peak current I_0 is defined as Qc divided by $3.5\sigma_{z,0}$. The normalized emittance is the geometric mean of the horizontal and the vertical values. The ~1 pC bunch length is initially compressed with velocity bunching (→) [11,12]. The magnetic compression is set to obtain a final peak current of 1.5 kA in all cases.

	PAL-1	**UCLA-1**	**LCLS-20**	**FERMI-100**
Q [pC]	1.6	1.0	20	100
σ_{t0} [ps]	1.2 → 0.002	1.6 → 0.002	1.3	1.2
I_0 [A]	0.4 → 200	0.2 → 140	5	25
C	1 x 7	1 x 11	10 x 34	5 x 13
γ_0	490	490	490	1470
γ_f	20550	20550	20550	2450
L_{FODO}, L_{tot} [m]	6, 680	6, 790	6, 790	12, 45
$\bar{\beta}$ [m]	35	35	35	25
$\tilde{\beta}$ [m]	3	3	3	3
Δ [μm]	200	200	200	100
$W_{\perp 0}$ [V/C/m^2]	1×10^{16}	1×10^{16}	1×10^{16}	17×10^{16}
ε_{n0} [mm mrad]	0.13	0.04	0.2	0.3
$CB_{n,0}$ [A/m^2]	8.9×10^{16}	9.4×10^{17}	3.74×10^{16}	1.67×10^{16}
$B_{n,f}$ (Eq. 6) [A/m^2]	**2.5×10^{16}**	**2.6×10^{17}**	**2.03×10^{16}**	**1.11×10^{16}**

REFERENCES

[1] S. Di Mitri, *Phys. Rev. ST Accel. Beams*, vol. 16, p. 050701, 2013.

[2] S. Di Mitri *et al.*, *Nucl. Instrum. Methods Phys. Res. A*, vol. 608, p. 19, 2009.

[3] E. Allaria *et al.*, *Nat. Photonics*, vol. 6, p. 699, 2012.

[4] E. Allaria *et al.*, *Nat. Photonics*, vol. 4, p. 2476, 2013.

[5] M. Dohlus, T. Limberg, and P. Emma, "Electron Bunch Length Compression," in International Committee for Future Accelerators Beam Dynamics Newsletter No.38, I. S. Ko, W. Chou (Eds.), p. 15, 2005, http://www-bd.fnal.gov/icfabd/Newsletter38.pdf

[6] E.L. Saldin *et al.*, *Nucl. Instrum. Methods Phys. Res. A*, vol. 398, p. 373, 1997.

[7] A.W. Chao, *Physics of Collective Beam Instabilities in High Energy Accelerators*, ISBN 0-471-55184-8, New York: Wiley, 1993.

[8] G. Guignard and J. Hagel, *Nucl. Instrum. Methods Phys. Res. A*, vol. 434, p. 179. 1999.

[9] T.O. Raubenheimer, *Phys. Rev. ST Accel. Beams*, vol. 3, p. 121002, 2000.

[10] P. Craievich, S. Di Mitri, and A.A. Zholents, *Nucl. Instr. and Meth. A*, vol. 604, p. 457, 2009.

[11] J.-H. Han, *Phys. Rev. ST Accel. Beams*, vol. 14, p. 050101, 2011.

[12] R.K. Li *et al.*, *Phys. Rev. ST Accel. Beams*, vol. 15, p. 090702, 2012.